Thermal Analysis of Electron-Beam Absorption in Low-Temperature Superconducting Films

M. I. Flik
Assistant Professor.
Mem. ASME

K. E. Goodson
Research Assistant.
Student Mem. ASME

Department of Mechanical Engineering,
Massachusetts Institute of Technology,
Cambridge, MA 02139

The absorption of an electron beam in a superconducting microbridge reduces its critical current, the maximum d-c electric current it can carry without resistance. A two-dimensional heat conduction analysis determines numerically the temperature field in the film caused by electron-beam heating, considering the nonlinear thermal boundary resistance between film and substrate. The method of Intrinsic Thermal Stability yields the critical current for this temperature field. The critical current predictions agree with experimental data from low-temperature scanning electron microscopy (LTSEM) with superconducting lead microbridges. The method developed in this study permits the quantitative prediction of LTSEM experiments, enhancing the value of this technique for the local characterization of superconducting films.

Introduction

Low temperature scanning electron microscopy (LTSEM) is a high-resolution technique for determining the spatial variation of properties in a sample at low temperatures (Huebener, 1988). A highly focused electron beam is scanned across the surface of the sample while a response signal is recorded simultaneously. The spatially dependent response provides information about sample properties such as chemical microstructure or surface inhomogeneity. One of the most useful applications of LTSEM is the characterization of superconducting films. The critical current of a superconducting microbridge is the maximum dc electric current it can carry without resistance. The absorption of the electron beam results in a temperature field that decreases the critical current of the microbridge. If a bias current is maintained in the microbridge that exceeds the reduced critical current, a voltage signal is measured along the microbridge.

In the past, LTSEM was applied to superconducting films in a qualitative manner. There is a need for a quantitative prediction of the critical current reduction resulting from the electron-beam absorption. Thermal analysis provides the theory to interpret LTSEM results quantitatively and determines the spatial extent of the temperature field that governs the resolution of LTSEM. The thermal interaction between superconducting devices, such as Josephson junctions, and semiconducting devices dictates a packing limit for the design of hybrid electronic circuitry (Flik and Hijikata, 1990). The experimental technique of LTSEM can be coupled with thermal analysis to investigate this limit. In the case of electron-beam pulses shorter than the time required to achieve thermal equilibrium, the comparison of thermal analysis with experimental data can assess the possibility of a nonequilibrium voltage response. Flik et al. (1990) applied this method to the case of laser-pulse absorption in high-temperature superconducting films.

Skocpol et al. (1974) studied the effect of Joule heating on current-voltage curves along a superconducting microbridge using a one-dimensional thermal model. Clem and Huebener (1980) determined the temperature field in a low-temperature superconducting microbridge resulting from the absorption of an LTSEM electron beam considering the finite width of the microbridge. Pavlicek et al. (1984) investigated the effect of modulating the beam power on the spatial resolution of the LTSEM technique using a one-dimensional thermal model. Flik and Tien (1990b) applied the criterion of Intrinsic Thermal Stability (Flik and Tien, 1990a) to the LTSEM experimental data of Stoehr et al. (1978) assuming an approximate point-symmetric temperature field.

This study predicts the temperature field and the reduced critical current in a superconducting microbridge resulting from electron-beam absorption. All of the aforementioned studies assumed a temperature-independent film thermal conductivity and a linear dependence of the heat flux from the film into the substrate on the film temperature. This work is the first thermal analysis of the absorption of an electron beam in a superconducting microbridge to investigate the importance of the variable thermal conductivity of the film, the nonlinear dependence of the heat flux between the film and substrate on the film temperature, and the influence of the beam-focus location. The theory of Intrinsic Thermal Stability is modified to account for the nonuniform distribution of the critical current in the microbridge cross section due to magnetic self-field effects. The critical current predictions are compared to experimental data of Stoehr et al. (1978) for a superconducting lead microbridge at 4.2 K on a sapphire substrate.

Electron-Beam Heat Source

Oatley (1972) and Wells (1974) gave summaries of the theory for the absorption of an electron beam in matter. Gross and Koyanagi (1985) showed that the spatial structure of the perturbation state of a lead superconducting film resulting from the absorption of an electron beam can be determined using the heat conduction equation. This section develops the distribution of heating power in the film used to model the absorption of the electron beam.

In electron-stopping theory applied to planar films, the electron fractional transmission $\eta(z)$ is the fraction of electrons incident on the surface of the film that pass through the plane parallel to the film surface at a depth z into the film. The electron mean energy $E_m(z)$ is the average energy of electrons transmitted through this plane. The electron mean range z_e is the depth into the film at which the quantity $E_m(z)$ is reduced to a value negligible compared to the electron initial energy, E_0. The mean energy, mean range, and fractional transmission of electrons with initial energies E_0 from 5 to 20 keV were measured by Cosslett and Thomas (1964a, 1964b) for aluminum, copper, silver, and gold films. The product of mass

Contributed by the Heat Transfer Division and presented at the 3rd ASME/JSME Joint Thermal Engineering Conference, Reno, Nevada, March 17–22, 1991. Manuscript received by the Heat Transfer Division January 3, 1991; revision received June 30, 1991. Keywords: Conduction, Cryogenics, Radiation Interactions.

density and electron mean range, ρz_e, varies slowly with atomic number Z for constant E_0 (Oatley, 1972). In the present analysis, the mean range of electrons in lead ($Z=82$) is determined using the correlation provided by Cosslett and Thomas (1964b) for gold films ($Z=79$):

$$\rho z_e = 1.1 \times 10^{-4} E_0^{3/2}, \quad (1)$$

where E_0 is in keV and ρz_e is in kg m^{-2}. This correlation is assumed to be accurate for the initial energies of $E_0=2$, 3, 5, 10, 20, and 30 keV used by Stoehr et al. (1978). Their microbridges were 1.1 μm in thickness. Using 11,340 kg m^{-3} for the density of lead, Eq. (1) yields electron mean ranges less than the film thickness for each value of E_0 except 30 keV, for which the electron mean range is 1.6 μm. For electron initial energies E_0 between 2 and 20 keV, the entire electron beam energy is absorbed within the film.

In the case of electrons with 30 keV initial energy, a portion of the electron-beam power is deposited in the substrate. The ratio of the electron-beam power absorbed within the substrate P_s to the total electron-beam power P for a film of thickness d is

$$\frac{P_s}{P} = \frac{E_m(z=d)}{E_0}\,\eta(z=d). \quad (2)$$

Cosslett and Thomas (1964a) correlated the electron fractional transmission to experimental data for values of E_0 from 15 to 25 keV, $\eta(z)=\exp(-19{,}000\,\rho z Z^{1/2}/E_0^2)$, where E_0 is in keV, and ρz is in kg m^{-2}. Cosslett and Thomas (1964b) showed that the electron mean energy at a depth z into the film satisfies $E_m(z)=E_0\,(1-z/z_e)^{1/2}$. Using these relations with $z=d=1.1$ μm and $z_e=1.6$ μm for 30 keV electrons and evaluating Eq. (2) yields $P_s=0.05\,P$. This fraction is neglected in the present analysis, allowing the use of a heat source entirely contained in the film to model the absorption of the electron-beam energy in the experiments of Stoehr et al. (1978).

The experiments of Stoehr et al. (1978) involved electron mean ranges that varied from 0.03 μm to 1.6 μm when calculated using Eq. (1). This indicates that the spatial extent of the heated volume was highly dependent on E_0. These experiments and later work (Stoehr and Huebener, 1979) showed that the variation of E_0 has a negligible effect on the critical current. This suggests that the points in the microbridge with a temperature dependent on E_0 were confined to a region with dimensions small compared to the microbridge width. This is confirmed in the present analysis by the comparison of temperature profiles in the microbridge determined using heat sources of varying size. In each case the maximum electron beam power in the experiments of Stoehr et al. (1978), $P=3$ mW, is uniformly distributed in a cylinder bounded by the top and bottom surfaces of the film. Cylinders with radii equal to the mean ranges of 2 keV and 30 keV electrons in lead are used for comparison. The variation by more than 2 percent in temperature between the two analyses is confined to a radius around the beam focus of 1.6 μm. This dimension is small compared to the microbridge width of 100 μm in the experiments of Stoehr et al. (1978). In the present analysis, the beam power is assumed to be deposited uniformly in the film within a cylinder of radius 0.87 μm, which is the mean range of 20 keV electrons. Depending on the value of E_0, the actual film temperature within a radius of 1.6 μm of the beam focus in the experiments of Stoehr et al. (1978) may have differed significantly from the temperature predicted in the present analysis. This error is not important for the calculation of the critical current because for all but the lowest beam powers it occurs at temperatures greater than the critical temperature of lead, $T_c=7.2$ K, the superconducting transition temperature. Regions of the film with temperature greater than 7.2 K do not contribute to the critical current of the film.

Film–Substrate Thermal Boundary Resistance

At low temperatures, the major obstacle to the flow of heat out of the film is the thermal boundary resistance between the film and substrate. Anderson (1981) reviewed the previous work on the low-temperature solid–solid thermal boundary resistance problem. Little (1959) developed the acoustic mismatch theory to predict the finite temperature drop measured at the interface of two solids at low temperatures. Acoustic mismatch theory predicts the rate of phonon transmission between two solids that have isotropic speeds of sound and share a smooth interface at which displacement and stress are continuous. Each solid is modeled as a Debye gas with phonons characteristic of a distinct temperature incident on the interface. If the temperature of each solid is much lower than its Debye temperature, Little (1959) found that the phonon heat flux q'' is

$$q'' = \kappa(T^4 - T_0^4) \quad (3)$$

where T and T_0 are the temperatures of the two solids and κ is a constant calculated from the velocities of longitudinal and transverse phonons in both solids and their mass densities (Anderson, 1981). Cheeke et al. (1976) tabulated parameters required for the calculation of κ for most interfaces. Acoustic mismatch theory is appropriate for the case of a metal film on a dielectric substrate because phonon transmission is the dominant mode of heat transfer. The value of κ used in the present analysis for the lead–sapphire interface, $\kappa=73$ W m^{-2}K^{-4}, was calculated by Cheeke et al. (1973) using

Nomenclature

A = area of film cross section, m^2
c = average sound velocity, m s^{-1}
d = film thickness, m
E_0 = initial electron energy, keV
E_m = mean energy of transmitted electrons, keV
h = heat transfer coefficient, W m^{-2}K^{-1}
h_P = Planck's constant = 6.62620×10^{-34} J s
I_c = microbridge critical current, A
I_{c0} = microbridge critical current at temperature T_0, A
J_c = local microbridge critical current density, A m^{-2}
k = thermal conductivity, W m^{-1}K^{-1}
k_{eff} = effective thermal conductivity along film, W m^{-1}K^{-1}
k_B = Boltzmann constant = 1.38062×10^{-23} J K^{-1}
m = electron rest mass = 9.10956×10^{-31} kg
P = electron-beam power, W
P_s = electron-beam power absorbed in substrate, W
q'' = heat flux from film to substrate, W m^{-2}
r = distance from beam focus, m
r_e = radius of cylinder directly heated by electron beam, m
T = film temperature, K
T_0 = bath temperature, K
T_c = superconducting film critical temperature, K
v_e = Fermi velocity, m s^{-1}
w = microbridge half-width, m
x = coordinate across microbridge width, m
x_f = beam focus location, m
y = coordinate along microbridge, parallel to current flow, m
Z = atomic number
z = coordinate normal to film, m
z_e = electron mean range, m
η = fraction of electrons transmitted
K_0 = modified Bessel function of the second kind of order zero
κ = constant, Eq. (3), W m^{-2} K^{-4}
ρ = mass density, kg m^{-3}

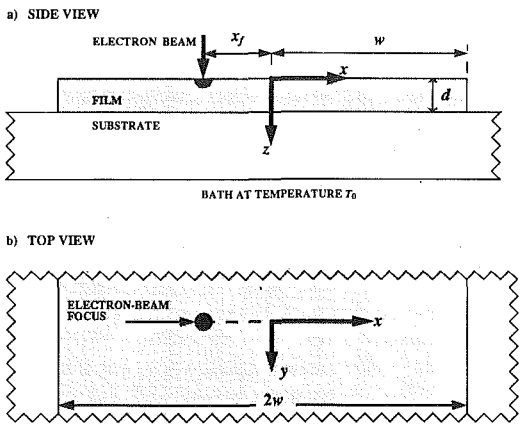

Fig. 1 Schematic of the absorption of an electron beam in a superconducting microbridge: (*a*) side view; (*b*) top view

a value of the Poisson ratio of 0.33 in both materials. Although Swartz and Pohl (1989) calculated $\kappa = 133$ W m^{-2}K^{-4} for a lead–sapphire interface using the actual Poisson ratios of the materials, the heat flux calculated using $\kappa = 73$ W m^{-2}K^{-4} is in better agreement with the experimental data of Cheeke et al. (1973) for lead films on sapphire.

The acoustic mismatch theory assumes that the interface between the two solids is smooth. This assumption is incorrect if the average phonon wavelength is comparable to or smaller than the characteristic dimension of roughness at the interface (Majumdar, 1991). At low temperatures the average phonon wavelength is of the order of $h_P c/k_B T$, where c is the speed of sound, h_P is Planck's constant, and k_B is the Boltzmann constant. This expression yields an average wavelength in lead at 4.2 K which is less than 3 percent of the thickness of the vapor-deposited films used by Stoehr et al. (1978), indicating that diffuse transmission might have affected the boundary resistance. The diffuse mismatch theory (Swartz and Pohl, 1989) predicts only a 6 percent increase in the thermal boundary resistance for lead–sapphire interfaces due to diffuse transmission compared to the value predicted by the acoustic mismatch theory. The effect of diffuse transmission on the accuracy of the acoustic mismatch theory is neglected in the present analysis.

Thermal Model and Numerical Analysis

Figure 1 illustrates the absorption of an electron beam in a thin-film microbridge of thickness d, 0.1 to 2 μm, and width $2w$, 10 to 500 μm, which has been deposited on a dielectric substrate. The bottom of the substrate is in contact with flowing liquid helium or nitrogen at the temperature T_0, and the top and the edges of the microbridge are exposed to a vacuum (Huebener, 1984). The electrons enter the microbridge at the focus of the electron beam that is 10 nm in diameter.

In the temperature range of the present analysis, 4.2 to 20 K, the thermal conductivity of the film material, lead, is highly dependent on temperature. Thermal conduction in metals is dominated by the motion of electrons and is limited by the scattering of electrons on defects and phonons. The rate of scattering of an electron on defects is independent of temperature and the rate of scattering of an electron on phonons increases with temperature. The thermal conductivity of a metallic superconductor such as lead is reduced in the superconducting state because superconducting electrons do not transport entropy. The thermal conductivity of superconducting lead is approximated by the following two polynomial functions fitted to experimental data given by Powell et al. (1966):

$$k(T) = 1352.7 - 407.57\ T + 38.894\ T^2, \quad 4.2 \le T < 7.2, \tag{4}$$

and

$$k(T) = 40244\ T^{-2} - 3946.0\ T^{-1} + 199.36 - 2.1698\ T, \quad 7.2 \le T \le 20, \tag{5}$$

where T is in K and k is in W m^{-1} K^{-1}.

If the mean free path of electrons in a metal film is of the order of or larger than the film thickness, the effective thermal conductivity along the film is less than that of a bulk sample. In a normal metal, the electron mean free path Λ is related to the thermal conductivity by (Kittel, 1986) $\Lambda = 3km v_e/(\pi^2 k_B^2 nT)$, where v_e is the Fermi velocity of the electrons, m is the electron rest mass, and n is the electron number density. At 7.2 K, the properties of lead are $k = 412$ W m^{-1} K^{-1}, $v_e = 0.50 \times 10^6$ m s^{-1}, and $n = 1.3 \times 10^{29}$ m^{-3}, yielding $\Lambda = 0.32$ μm, which is of the order of the film thickness, 1.1 μm. For $\Lambda < d$, the effective conductivity along the film is approximately (Flik and Tien, 1990c) $k_{\text{eff}} = (1 - 2\Lambda/(3\pi d))\ k$, yielding $k_{\text{eff}} = 0.94\ k$ for the 1.1 μm film with $\Lambda = 0.32$ μm. This size effect is neglected in the present analysis because of its small estimated magnitude.

The scanning speed of an electron beam is typically 0.1 m s^{-1} (Huebener, 1984). Steady thermal analysis in the frame of reference of the moving electron beam has been shown to be appropriate for the experiments of Stoehr et al. (1978) by Flik and Tien (1990b) due to the large thermal diffusivity of lead at 4.2 K, 0.19 m^2 s^{-1}, and the small scanning velocity. This approach is confirmed by consideration of the thermal relaxation time of 2 μs measured in pulsed electron beam experiments by Stoehr et al. (1978). The scanning beam traveled 0.2 μm in this time, which is small compared to the film thickness, $d = 1.1$ μm, the smallest dimension of the microbridge.

The top and sides of the microbridge are insulated by vacuum space and a radiation shield, yielding adiabatic boundary conditions at these surfaces. The energy from the electron beam travels through the film, across the film–substrate interface, through the substrate, and across the substrate–bath interface before it is absorbed by the flowing liquid helium. The thermal boundary resistance at the substrate–bath interface is neglected. Because of the nonlinear film–substrate boundary resistance and the variable thermal conductivity of both sapphire and lead at low temperatures, the relative importance of the remaining thermal resistances is highly dependent on temperature.

The substrate is modeled as isothermal at the bath temperature because of its low thermal resistance relative to the lead–sapphire boundary resistance. The error incurred by this assumption for a film temperature T is estimated by solving the steady, constant conductivity, two-dimensional heat equation in the substrate using separation of variables. The substrate is 1 mm thick (Stoehr et al., 1978) and 10 mm wide. The top of the slab is adiabatic except for the portion covered by the film, where the heat flux is approximated using Eq. (3) with T as the film temperature and T_0 as the bath temperature. The edges and bottom of the substrate are at the bath temperature. Using the minimum conductivity of sapphire between 4.2 K and 20 K, the largest temperature difference between the top and bottom surfaces of the substrate is found to be less than 10 percent of the total temperature difference between the film and the bath for film temperatures less than 20 K. For larger film temperatures the neglect of the thermal resistance of the substrate results in a significant underprediction of the film temperature.

Using Eq. (3), the temperature-dependent conductance h between the film and substrate is $h = \kappa(T^4 - T_0^4)/(T - T_0)$. Using this expression for h and Eqs. (4) and (5) for k, the Biot number $\text{Bi} = hd/k$ for conduction normal to the film is less than 0.01 for film temperatures less than 21 K. Therefore,

temperature gradients in the film in the z direction are neglected, resulting in a two-dimensional analysis of heat conduction in the film. The two-dimensional energy equations in the film are

$$\frac{\partial}{\partial x}\left(k\frac{\partial T}{\partial x}\right)+\frac{\partial}{\partial y}\left(k\frac{\partial T}{\partial y}\right)-\frac{\kappa}{d}(T^4-T_0^4)+\frac{P}{\pi d(r_e)^2}=0; \quad (6)$$

$$(x_f-x)^2+y^2\le(r_e)^2$$

and

$$\frac{\partial}{\partial x}\left(k\frac{\partial T}{\partial x}\right)+\frac{\partial}{\partial y}\left(k\frac{\partial T}{\partial y}\right)-\frac{\kappa}{d}(T^4-T_0^4)=0; \quad (7)$$

$$(x_f-x)^2+y^2>(r_e)^2,$$

where r_e is the radius of a cylinder of uniform power absorption in the film centered around the line normal to the film surface through the point $(x=x_f, y=0)$, which is set at the mean range of 20 keV electrons in lead, $r_e=0.87$ μm. The boundary conditions are

$$\frac{\partial T}{\partial x}=0 \text{ for } x=-w \text{ and } x=w \quad (8)$$

and

$$T\to T_0 \text{ for } y\to+\infty \text{ and } y\to-\infty. \quad (9)$$

The governing equations are solved numerically using the central difference technique described by Patankar (1980). The energy balance is verified globally in the microbridge and locally at each grid element by independent computational routines. The repeatability of the solution for different initial temperature distributions is verified. For the case of very narrow microbridges the numerical solution matches an independently computed solution of the one-dimensional heat transfer problem. If the film-substrate heat flux given by Eq. (3) is linearized to $q''=4\kappa T_0^3(T-T_0)$, the computed solution for very wide microbridges approaches the point-symmetric closed-form solution of Flik and Tien (1990b),

$$T(r)=T_0+\frac{P}{2\pi kd}\,\mathrm{K}_0\left[\frac{r}{\sqrt{kd/4\kappa T_0^3}}\right], \quad (10)$$

where r is the distance from the beam focus and K_0 is the modified Bessel function of the second kind of order zero.

Microbridge Critical Current

The critical current of a microbridge decreases with increasing temperature and is reduced to zero at the critical temperature of the superconductor, T_c. Flik and Tien (1990a) computed the critical current of a microbridge in the presence of a temperature field. If J_c is the local critical current density at a point in the microbridge resulting from the temperature T at that point, the critical current of a cross section is

$$I_c=\int_A J_c\,dA, \quad (11)$$

where dA is an area element in the bridge cross section A normal to the direction of current flow. The critical current of the entire bridge is the minimum of the critical currents of all cross sections. Flik and Tien (1990b) determined the critical current of the microbridge by assuming a uniform distribution of critical current density in an isothermal bridge. This approach neglects the complex interaction of geometry and magnetic field in planar superconducting microbridges, which results in a nonuniform distribution of critical current density (Edwards and Newhouse, 1962). The present work considers the nonuniform distribution of critical current.

The dependence of J_c on temperature for a type-I superconducting film like lead deposited on a cylinder is (Newhouse, 1964)

$$\frac{J_c(T)}{J_c(T_0)}=\frac{\left[1-\left(\frac{T}{T_c}\right)^2\right]^{3/2}\left[1+\left(\frac{T}{T_c}\right)^2\right]^{1/2}}{\left[1-\left(\frac{T_0}{T_c}\right)^2\right]^{3/2}\left[1+\left(\frac{T_0}{T_c}\right)^2\right]^{1/2}}. \quad (12)$$

where $J_c(T_0)$ is the critical density of the film when it is isothermal at T_0. Although Eq. (12) predicts the temperature dependence of the uniform critical current density of a film deposited on a microbridge, it is assumed in the present analysis to predict the temperature dependence of the local critical current density of a planar microbridge in terms of the local value of $J_c(T_0)$. The variation of $J_c(T_0)$ with x in a planar microbridge is determined using the relation of Newhouse (1964) for the supercurrent density $J(x)$ at a position x in the cross section of an isothermal microbridge,

$$J(x)=\frac{I}{2\pi d[w^2-x^2]^{1/2}}, \quad (13)$$

where I is the bias current and w is the half-width of the microbridge. Equation (12) is valid for films of thickness much larger than London penetration depth. The London penetration depth characterizes the exponential decay of magnetic field strength from the edge of a superconductor into its interior in the case of an externally applied magnetic field. Equation (13) is valid for microbridges that are much wider than they are thick, yet have thickness much larger than London penetration depth. These criteria are satisfied by the lead microbridges used by Stoehr et al. (1978), which had a width $2w$ of 100 μm, a thickness d of 1.1 μm, and a London penetration depth of 0.051 μm.

In the present analysis, the local critical current density at a point in the film is assumed to depend only on the x coordinate and the temperature at that point, $J_c=J_c(T,x)$. Equation (13), with I_{c0} substituted for I and $J_c(T_0,x)$ substituted for $J_c(x)$, is assumed to give the distribution of local critical current density in the bridge when it is isothermal at temperature T_0. The critical current I_{c0} of the unirradiated microbridge, which was isothermal at the bath temperature, was measured to be $I_{c0}=0.869$ A by Stoehr et al. (1978). Equation (12), with $J_c(T_0,x)$ substituted for $J_c(T_0)$ and $J_c(T,x)$ substituted for $J_c(T)$, is assumed to determine the local critical current density in the microbridge as a function of the local temperature T and the local critical current density at that point at the bath temperature. The effects of geometry and temperature on the local critical current density are assumed to be independent.

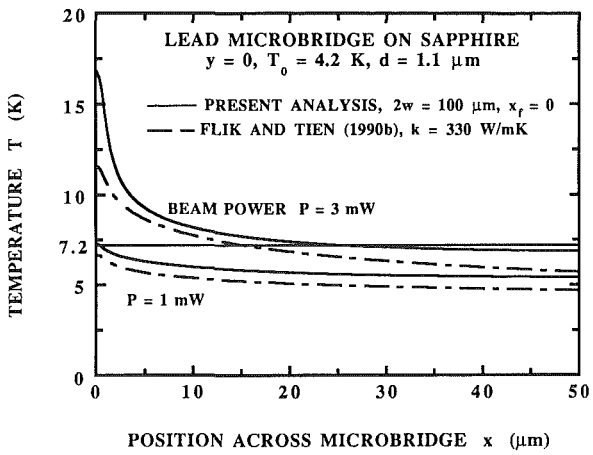

Fig. 2 Comparison of the present analysis with the closed-form solution of Flik and Tien (1990b)

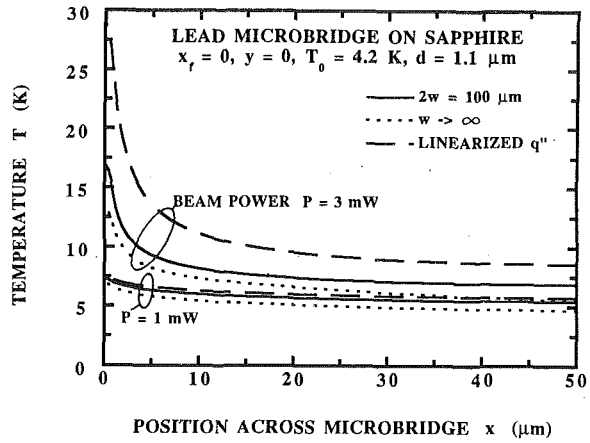

Fig. 3 Influence of the assumptions of infinite microbridge width and linearized film-substrate heat flux

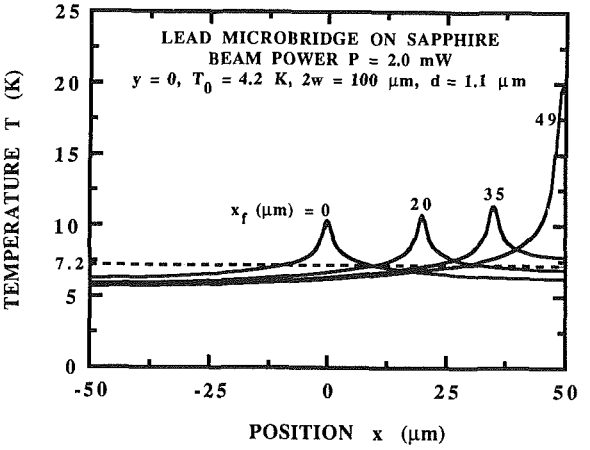

Fig. 4 Temperature profiles across the microbridge for different electron-beam focus locations

Equations (11), (12), and (13) are combined with the temperature-field solution from the thermal analysis, $T(P,x_f;x,y)$, to compute the critical current in each cross section of the microbridge. The critical current of cross section y during the absorption of an electron beam of power P, which is focused on the microbridge at the coordinates $(x=x_f, y=0)$, is given by

$$I_c(P,x_f,y)=\int_{-w}^{w}\frac{I_{c0}}{2\pi[w^2-x^2]^{1/2}}\times\frac{\left[1-\left(\frac{T(P,x_f;x,y)}{T_c}\right)^2\right]^{3/2}\left[1+\left(\frac{T(P,x_f;x,y)}{T_c}\right)^2\right]^{1/2}}{\left[1-\left(\frac{T_0}{T_c}\right)^2\right]^{3/2}\left[1+\left(\frac{T_0}{T_c}\right)^2\right]^{1/2}}dx. \tag{14}$$

Equation (14) assumes that, in the presence of the electron beam, the current in the film redistributes itself such that it makes the best use of the available current density distribution, which is different from that given by Eq. (13) due to the temperature field. A voltage along the bridge appears only if the bridge current exceeds I_c given by Eq. (14) for some y.

The temperature along lines of constant x peaks at the cross section directly under the beam focus, $y=0$. This cross section limits the critical current of the entire bridge. For given bridge dimensions and film and substrate materials, the overall microbridge critical current I_c depends on the beam power P and beam focus location x_f. Stoehr et al. (1978) measured the critical current as a function of the power of the electron beam, which scanned the entire width of the microbridge. The present analysis shows that for different beam powers the maximum reduction of the microbridge critical current occurred at different locations of the beam focus. Equation (14) predicts the critical current in cross section y resulting from the absorption of a beam of power P at the beam focus location x_f. To predict the experimental results obtained using a scanning beam, it is necessary to determine the critical current in the cross section $y=0$ for all beam focus locations at each beam power. The minimum value of I_c for all beam focus locations at each beam power predicts the critical current measured by Stoehr et al. (1978) at that beam power,

$$I_c(P)=\text{MIN}[I_c(P,x_f,y=0)],\quad 0\le x_f\le w. \tag{15}$$

Results and Discussion

The microbridge cross section whose critical current is most reduced by the electron beam is located at $y = 0$. Since temperature differences in the z direction in the film are neglected, temperature profiles in this cross section are presented in Figs. 2-4 with respect to the x coordinate only. Figure 2 compares temperature profiles obtained in the present analysis to those obtained using the theory of Flik and Tien (1990b), which was derived for a microbridge of infinite width with a temperature-independent thermal conductivity. In addition, the heat flux between the film and substrate was linearized to the form

$$q''=4\kappa T_0^3(T-T_0). \tag{16}$$

The thermal conductivity of lead at 4.2 K, 330 W m^{-1} K^{-1}, and a heat absorption cylinder of radius 0.87 μm are used in evaluating the closed-form solution. The critical temperature of lead, $T_c=7.2$ K, is shown in Fig. 2 to indicate the importance of the error in temperature of the closed-form solution for the calculation of the critical current.

Since the closed-form solution applies to microbridges of infinite width it underpredicts the temperature field in a microbridge of finite width. The importance of this effect increases with an increase in the ratio of the film thermal healing length, $(kd/h)^{1/2}$, to the distance from the beam focus to the nearest microbridge edge. Using 330 W m^{-1} K^{-1} for k and 2.1×10^4 W m^{-2} K^{-1} for h yields a linearized thermal healing length of 130 μm, which is larger than the microbridge half-width of 50 μm. The linearization of Eq. (3) given by Eq. (16) is appropriate only for film temperatures T such that $(T-T_0)/T_0\ll1$. If this condition is not satisfied, Eq. (16) underpredicts the flow of heat into the substrate.

The good performance of the closed-form solution results from two compensating assumptions, whose relative importance is shown in Fig. 3. The solid curves indicate the exact solution of the present analysis. The other curves indicate solutions of the present analysis either for bridges of infinite width or for microbridges with linearized heat flux. Both assumptions are justified at the beam power of 1 mW. At 3 mW the linearization is the worst simplification, resulting in an error in temperature of more than 50 percent at $x=4.3$ μm. The error due to the heat flux linearization increases more rapidly with beam power than the error due to the infinite microbridge width assumption.

The effect of neglecting the temperature dependence of the thermal conductivity of lead is also investigated. If the thermal conductivity of lead is assumed to be constant at its value at 4.2 K, 330 W m^{-1}K^{-1}, the temperature is underpredicted near the beam focus. This is because the film thermal conductivity given by Eqs. (4) and (5) is actually much lower than 330 W m^{-1}K^{-1} in the regions with higher temperature.

Figure 4 shows the effect of varying the beam focus location on the temperature profiles for a single beam power. The maximum temperature of the film and the spatial extent of

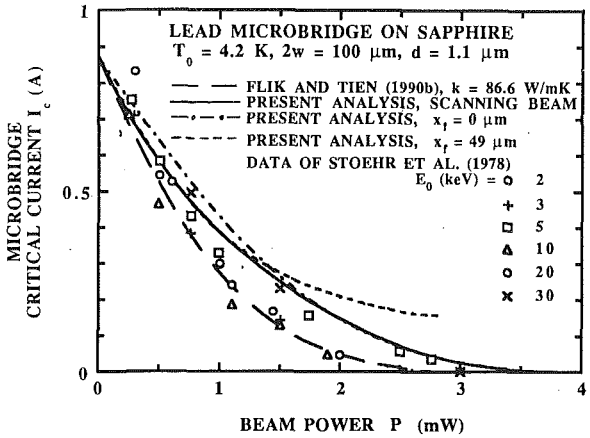

Fig. 5 Comparison of theory with experimental data for the dependence of the critical current on the beam power

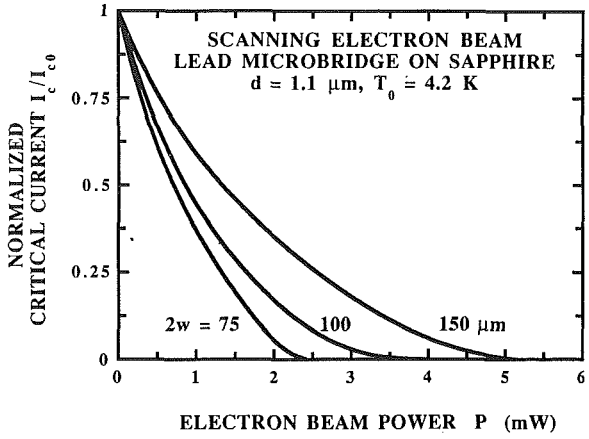

Fig. 6 Dependence of the critical current on the beam power for three microbridge widths

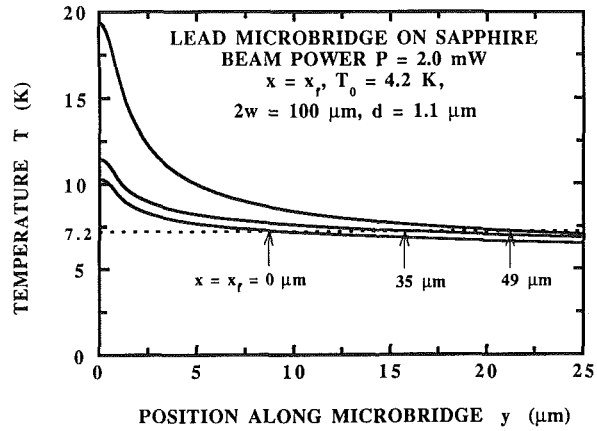

Fig. 7 Longitudinal temperature profiles for different beam focus locations

the portion of the film with temperature above the critical temperature T_c are highly dependent on the beam focus location. While the maximum temperature increases as the beam focus location approaches the adiabatic edge of the microbridge, the width of the portion of the film above the critical temperature reaches a maximum for a beam focus location in the interior of the microbridge. The beam focus location has a strong influence on the microbridge critical current because the critical current density distribution in the bridge cross section given by Eq. (13) peaks at the bridge edges.

Figure 5 compares the present solution for the critical current as a function of the beam power to the closed-form solution of Flik and Tien (1990b) and to the experimental data of Stoehr et al. (1978). The closed-form solution of Flik and Tien (1990b) was calculated using a thermal conductivity of lead of 86.6 W m^{-1} K^{-1}. The theory of Flik and Tien (1990b) is in agreement with the experimental data. This is due in part to the competing effects of the assumptions of linearized film–substrate heat flux and infinite microbridge width. This theory cannot be expected to predict other data as well, in particular for the cases of very narrow films and large values of $(T-T_0)/T_0$.

Stoehr et al. (1978) varied both the electron beam voltage and the electron beam current to control the beam power. The electron initial energy E_0, which increases linearly with the beam voltage, is of negligible importance to the measured critical current. For low beam powers, a beam focused near the edge of the microbridge ($x_f = 49$ μm) has the greatest effect on the critical current, the density of which is assumed to be greatest near the microbridge edges. In contrast, an electron beam focused at the center of the microbridge ($x_f = 0$ μm) requires less power to make the entire width of the microbridge normal than a beam focused at the edge. The electron beam is scanned across the entire width of the microbridge, and each beam focus location determines at some beam power the microbridge critical current. The solid curve for the scanning beam is the minimum envelope of curves relating critical current to beam power for all beam focus locations. Figure 6 shows this minimum envelope for three values of the microbridge width $2w$. The ordinate of this graph is the ratio of the microbridge critical current to the critical current of the unirradiated microbridge, I_c/I_{c0}. The normalized critical current increases for a given beam power with increasing microbridge width. The beam power at which the critical current in the microbridge is reduced to zero increases with increasing microbridge width.

Figure 7 shows temperature profiles in planes parallel to the flow of current and normal to the film surface. For each beam focus location x_f the temperature profile is given for the plane parallel to the flow of electric current that contains the line $x = x_f$, $z = 0$. The arrows show for each beam focus location the value of y at which the temperature is equal to the critical temperature. This figure indicates that the longitudinal extent of the normally resistive region in the microbridge increases as the beam focus approaches the microbridge edge. This helps to explain the shape of the voltage response obtained by Stoehr et al. (1978) due to scanning the electron beam across the microbridge width at constant power with a constant bias current in the microbridge. The greater longitudinal extent of the normal region, along with the maxima in the critical current density distribution at the microbridge edges, resulted in the peaks in voltage response when the beam was focused near the microbridge edges.

Concluding Remarks

If the characteristic dimension of the film volume directly heated by the electron beam is much smaller than the width of the microbridge, the variation of the distribution of heating intensity within that volume has little effect on the microbridge critical current. Thermal analysis of a microbridge of width of the order of or smaller than its linearized thermal healing length, $(kd/h)^{1/2}$, must consider the finite microbridge width. A linearization of the heat flux from the film to the substrate is appropriate if the temperature T in the film satisfies $(T-T_0)/T_0 \ll 1$, where T_0 is the substrate temperature. The error due to this linearization increases rapidly with the power of the electron beam.

The voltage response in a superconducting microbridge is determined by the beam power and focus location and the bias

current in the microbridge. The present thermal analysis becomes appropriate for investigation of the voltage response if Joule heating is incorporated into the energy balance and the potential for normal-zone thermal propagation is considered. Prediction of the voltage response requires experimental data for the resistivity in the microbridge as a function of its temperature and bias current.

The theory in the present analysis for the prediction of critical currents in low-temperature superconducting microbridges is an idealization of the complex interaction of electrical current, magnetic field, and temperature with the microbridge geometry. A theory for the case of epitaxial high-temperature superconducting microbridges must consider the anisotropy of those materials and the effects of flux creep and grain boundaries. There is a need for simple, yet accurate models that describe the behavior of supercurrent in specific geometries with temperature fields. The agreement of the predicted critical current with experimental data in the present work shows that the method of Intrinsic Thermal Stability has promise for the prediction of the critical current of high-temperature superconductors in the presence of thermal disturbances.

Acknowledgments

The authors thank Professor J. L. Smith of the Massachusetts Institute of Technology for his commentary and criticism. M.I.F. acknowledges the support of the Lynde and Harry Bradley Foundation through a Career Development Chair and K.E.G. the support of the Office of Naval Research through an academic fellowship.

References

Anderson, A. C., 1981, "The Kapitza Thermal Boundary Resistance Between Two Solids," in: *Non-Equilibrium Superconductivity, Phonons, and Kapitza Boundaries*, K. E. Gray, ed., Plenum Press, New York, pp. 1–30.

Cheeke, J. D. N., Hebral, B., and Martinon, C., 1973, "Transfert de Chaleur entre Deux Solides en Dessous de 100 K," *J. Phys. (Paris)*, Vol. 34, pp. 257–272.

Cheeke, J. D. N., Ettinger, H., and Hebral, B., 1976, "Analysis of Heat Transfer Between Solids at Low Temperatures," *Can. J. Phys.*, Vol. 54, pp. 1749–1765.

Clem, J. C., and Huebener, R. P., 1980, "Applications of Low-Temperature Scanning Electron Microscopy to Superconductors," *J. Appl. Phys.*, Vol. 51, pp. 2764–2773.

Cosslett, V. E., and Thomas, R. N., 1964a, "Multiple Scattering of 5–30 keV Electrons in Evaporated Metal Films: I. Total Transmission and Angular Distribution," *Br. J. Appl. Phys.*, Vol. 15, pp. 883–907.

Cosslett, V. E., and Thomas, R. N., 1964b, "Multiple Scattering of 5–30 keV Electrons in Evaporated Metal Films: II. Range-Energy Relations," *Br. J. Appl. Phys.*, Vol. 15, pp. 1283–1300.

Edwards, H. H., and Newhouse, V. L., 1962, "Superconducting Film Geometry with Strong Critical Current Asymmetry," *J. Appl. Phys.*, Vol. 33, pp. 868–874.

Flik, M. I., and Hijikata, K., 1990, "Approximate Thermal Packaging Limit for Hybrid Superconductor-Semiconductor Electronic Circuits," *Heat Transfer 1990*, G. Hetsroni, ed., Hemisphere, New York, Vol. 2, pp. 319–324.

Flik, M. I., Phelan, P. E., and Tien, C. L., 1990, "Thermal Model for the Bolometric Response of High-T_c Superconducting Films to Optical Pulses," *Cryogenics*, Vol. 30, pp. 1118–1128.

Flik, M. I., and Tien, C. L., 1990a, "Intrinsic Thermal Stability of Anisotropic Thin-Film Superconductors," ASME JOURNAL OF HEAT TRANSFER, Vol. 112, pp. 10–15.

Flik, M. I., and Tien, C. L., 1990b, "Intrinsic Thermal Stability for Scanning Electron Microscopy of Thin-Film Superconductors," *J. Appl. Phys.*, Vol. 67, pp. 362–370.

Flik, M. I., and Tien, C. L., 1990c, "Size Effect on the Thermal Conductivity of High-T_c Thin-Film Superconductors," ASME JOURNAL OF HEAT TRANSFER, Vol. 112, pp. 872–881.

Gross, R., and Koyanagi, M., 1985, "Effect of Electron-Beam Irradiation on Superconducting Films," *J. Low Temp. Phys.*, Vol. 60, pp. 277–295.

Huebener, R. P., 1984, "Applications of Scanning Electron Microscopy," *Rep. Prog. Phys.*, Vol. 47, pp. 175–220.

Huebener, R. P., 1988, "Scanning Electron Microscopy at Very Low Temperatures," in: *Advances in Electronics and Electron Physics*, P. W. Hawkes, ed., Academic Press, New York, Vol. 70, pp. 1–79.

Kittel, C., 1986, *Introduction to Solid State Physics*, Wiley, New York, p. 150.

Little, W. A., 1959, "The Transport of Heat Between Dissimilar Solids at Low Temperatures," *Can. J. Phys.*, Vol. 37, pp. 334–349.

Majumdar, A., 1991, "Effect of Interfacial Roughness on Phonon Radiative Heat Conduction," *Proceedings of the ASME/JSME Thermal Engineering Joint Conference*, Reno, NV, Vol. 4, pp. 99–110.

Newhouse, V. L., 1964, *Applied Superconductivity*, Wiley, New York, pp. 109–112, 122–126.

Oatley, C. W., 1972, *The Scanning Electron Microscope, Part 1: The Instrument*, Cambridge University Press, Cambridge, United Kingdom, pp. 134–167.

Patankar, S. V., 1980, *Numerical Heat Transfer and Fluid Flow*, Hemisphere, New York, pp. 41–77.

Pavlicek, H., Freytag, L., Seyfert, H., and Huebener, R. P., 1984, "Resolution Limit Due to Thermal Effects in Low-Temperature Scanning Electron Microscopy," *J. Low Temp. Phys.*, Vol. 56, pp. 237–257.

Powell, R. W., Ho, C. Y., and Liley, P. E., 1966, *Thermal Conductivity of Selected Materials*, Part 2, U.S. Government Printing Office, Washington, pp. 19, 175–181.

Skocpol, W. J., Beasley, M. R., and Tinkham, M., 1974, "Self-Heating Hotspots in Superconducting Thin-Film Microbridges," *J. Appl. Phys.*, Vol. 45, pp. 4054–4066.

Stoehr, P. L., Noto, K., and Huebener, R. P., 1978, "Superconducting Microbridges Under Irradiation With an Electron Beam," *J. Phys. (Paris)*, Coll. C6, Suppl. 8, Vol. 39, pp. C6/527–528.

Stoehr, P. L., and Huebener, R. P., 1979, "Two-Dimensional Imaging of the Resistive Voltage Changes in a Superconductor Caused by Irradiation With an Electron Beam," *J. Low Temp. Phys.*, Vol. 37, pp. 277–287.

Swartz, E. T., and Pohl, R. O., 1989, "Thermal Boundary Resistance," *Rev. Mod. Phys.*, Vol. 61, pp. 605–668.

Wells, O. C., 1974, *Scanning Electron Microscopy*, McGraw-Hill, New York, pp. 37–68.